Design and Implementation of Smart Home Control Systems Based on Wireless Sensor Networks and Power Line Communications

Mingfu Li and Hung-Ju Lin

***Abstract*—Wireless sensor networks (WSNs) and power line communications (PLCs) are used in this work to implement a smart home control network. The goals are to reduce the impact of wireless interference on a smart home control network and unnecessary energy consumption of a smart home. An isolated WSN with one coordinator, which is integrated into the PLC transceiver, is established in each room. The coordinator is responsible for transferring environmental parameters obtained by WSNs to the management station via PLCs. The control messages for home appliances are directly transferred using PLCs rather than WSNs. According to the experimental results, the impact of wireless interference on the proposed smart home control network is substantially mitigated. Additionally, a smart control algorithm for lighting systems and an analysis of the illumination of a fluorescent lamp were presented. The energy saving of lighting systems relative to those without smart control was evaluated. Numerical results indicate that the electricity consumption on a sunny or cloudy day can be reduced by at least 40% under the smart control. Moreover, a prototype for the proposed smart home control network with the smart control algorithm was implemented. Experimental tests demonstrate that the proposed system for smart home control networks is practically feasible and performs well.**

***Index Terms*—Appliance control, energy saving, power line communications (PLCs), smart homes, smart lighting control, wireless sensor networks (WSNs).**

I. Introduction

NUMEROUS studies [1]–[3] have shown that smart homes or intelligent buildings can use energy more efficiently than traditional buildings. Thus, several researchers have advocated building smart homes for reducing energy consumption. Almost all proposed smart home architectures in the literature adopt the wireless sensor network (WSN) as the dominant technology [3]–[9]. The WSN, rather than Wi-Fi, has been popularly employed for remote control and monitoring applications [10]–[13] because it has a low cost and consumes little power. However, several problems in the construction of smart homes with WSNs are yet to be solved.

The studies [14] and [15] presented a comprehensive review of problems related to the development of smart homes with WSN technologies. For WSNs, if the network coverage exceeds a certain range or the network environment cannot provide a line-of-sight transmission, then high transmission error and data loss rates may occur. Hence, designing a scalable network infrastructure for WSNs is very important. Although several techniques have been proposed to improve WSN connectivity [16], the challenge of improving connectivity in WSNs still exists. Furthermore, WSNs and WLANs both operate in the 2.4-GHz industrial, science and medical band. Experimental results [17]–[19] have demonstrated that Wi-Fi networks and WSNs may function together even if they operate in the same frequency band. However, inevitable wireless interference and packet losses may occur in WSNs. To solve this problem, some methods have been proposed for interference avoidance [19] or coordinating such a heterogeneous network environment [20]. However, a more effective interference immunity solution for WSNs remains to be found. To resolve the issue of wireless interference, the WSN is integrated herein with the power line communication (PLC) technology to realize a smart home control network.

Well-known PLC technologies include X10 [21], CEBus [22], LonWorks [23], and HomePlug [24]. According to the relevant specifications, PLC can be categorized as broad-band PLC (B-PLC) or narrow-band PLC (N-PLC) [25]. X10, CEBus, and LonWorks are forms of N-PLC, while HomePlug is a form of B-PLC. B-PLC uses a higher frequency band (1.8 to 250 MHz) and has a wider spectrum. Hence, B-PLC can offer a higher data rate and lower network latency than N-PLC. However, N-PLC has a low cost of deployment and the ability to communicate across the transformer. Recently, multicarrier-based N-PLC technologies such as Powerline Intelligent Metering Evolution, G3-PLC, IEEE 1901.2, and ITU-T G.hnem have been proposed to offer higher data rates [25]. Some recent proposals [26]–[30] for smart homes or control networks have adopted PLC technologies to build the communication systems. One of the most important benefits to using PLCs in this work is a less relevant packet failure rate for WSNs.

One of the main purposes of smart homes is to reduce energy consumption. To achieve this goal, smart controls must be implemented in a smart home. Additionally, smart lighting control systems must consider the contribution of natural light

Manuscript received March 13, 2014; revised June 16, 2014, August 9, 2014, and October 7, 2014; accepted November 18, 2014. Date of publication December 10, 2014; date of current version May 15, 2015. This work was supported by the Ministry of Science and Technology of Taiwan under Grant NSC100-2221-E-182-068 and Grant NSC102-2221-E-182-002-MY2.

M. Li is with the Department of Electrical Engineering, School of Electrical and Computer Engineering, College of Engineering, Chang Gung University, Tao-Yuan 33302, Taiwan (e-mail: mfli@mail.cgu.edu.tw).

H.-J. Lin is with the Taiwan Power Company, Taipei 10016, Taiwan (e-mail: m9921017@stmail.cgu.edu.tw).

Color versions of one or more of the figures in this paper are available online at http://ieeexplore.ieee.org.

Digital Object Identifier 10.1109/TIE.2014.2379586

(daylight). Therefore, several works [31]–[33] suggested that daylight can substitute for partial electrical lighting in commercial or institutional buildings. Sensors and smart controllers enable daylight to reduce the power used to run electrical lighting and to sufficiently illuminate an office. Although many ideas about smart lighting control for energy saving in smart homes have been proposed, a practical smart lighting control system with high reliability and control accuracy remains to be found. An accurate and reliable lighting control system must have a robust environmental illumination gathering system. However, only few papers [11] considered the impact of packet failure on the performance of smart control systems. According to the simulation results in [11], packet failure not only deteriorates the final control achievement but also slows down the speed of approaching the control goal. Accordingly, constructing the communication network with a low packet failure rate to support smart control systems is extremely required.

The novelty and contributions of this paper are summarized as follows. First, the scalable architecture that combines WSN and PLC technologies for the smart home control network is presented. The proposed network infrastructure can considerably mitigate the impact of radio interference and simplify node placement in WSNs. The proposed smart home control system includes the environmental information gathering, communication, and appliance control subsystems. It also allows users to remotely monitor and control home appliances using the Internet and the web-based management system. Second, a smart control algorithm for lighting systems in smart homes or intelligent buildings is proposed. Third, a prototype of the smart home control network with the proposed smart lighting control algorithm is developed, tested, and evaluated.

The rest of this paper is organized as follows. Section II discusses different architectures of smart home control networks. Performance comparisons between different network architectures are made. Section III presents a smart lighting control algorithm and evaluates the energy saving ratio of the smart home under smart control. Section IV describes issues related to the implementation of the proposed smart home control network. A prototype of the proposed system is implemented and tested. Finally, Section V provides the concluding remarks.

II. Design and Performance Evaluation of Smart Home Control Networks

A. Architectural Design of Smart Home Control Networks

Fig. 1 displays the proposed architecture of the smart home control network. Three rooms in a smart home are considered as an example. Each home appliance is equipped with a PLC transceiver, which can directly receive commands to control the home appliance and send replies about the state of the home appliance to the management station. An isolated WSN, which includes various sensor nodes and one coordinator that is integrated into the PLC transceiver, is deployed in each room to collect environmental information, such as temperature, illumination, humidity, and other information.

In the proposed architecture, WSNs are responsible for collecting environmental parameters and transmitting them to

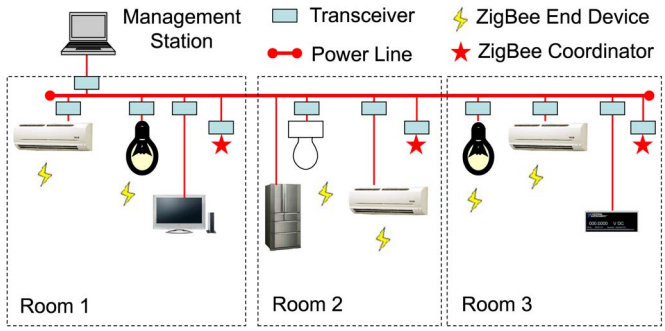

Fig. 1. Architecture of proposed smart home control network.

WSN coordinators, while PLCs are used as a network backbone to connect all WSN coordinators and transfer the collected environmental data to the management station and the control messages to home appliances. The proposed design in this paper is quite different from that of conventional WSN-based smart homes [3]–[5], [8], [9], [11] in which the control commands for home appliances are transferred using WSNs. The main purposes of the proposed design are to extend the coverage of a smart home control network and mitigate the impact of wireless interference on the WSN data gathering subsystem. A similar solution that also combines wireless and PLC technologies is the INSTEON technology [30]. However, the wireless technology in INSTEON is mainly used to relay control commands and extend the scale of a control network, rather than gather environmental information for smart controls.

Another issue in a smart home is how a user can remotely connect and get access to a smart home control network. One method uses a web-based service for sharing information with the management station at the remote site via Internet [34], [35]. Another access method adopts the mobile cellular service architecture [36], [37], such as GSM, GPRS, or 3G/4G. Thus, there is no difficulty to remotely monitor the smart home and control it in real time via the Internet.

B. Performance of WSNs Under Interference of WLANs

Wi-Fi networks are extensively deployed around the world, and Wi-Fi signals degrade the performance of WSNs with low power consumption [18], [19]. To study the impact of WLAN interference on the performance of WSNs, this study investigates the performance of ZigBee WSNs under different jamming traffic loads from a Wi-Fi network. The performance of WSNs is compared across different network architectures, which are displayed in Fig. 2.

Fig. 2(a) depicts the conventional infrastructure of WSNs with relay nodes (pure WSN architecture). The environment with three rooms in a line is considered here. The notebook in Room A is used to receive the jamming traffic (UDP traffic) from the Wi-Fi access point (AP). To solve the problem of the obstacles in the form of walls between rooms, several relay nodes for the WSN are allocated among the rooms to ensure that all ZigBee end devices can communicate with the coordinator in Room A. The polling rate of each relay node is set to 0.5 s. Fig. 2(b) presents the proposed infrastructure that includes the WSN plus PLC. Each room is allocated one WSN coordinator,

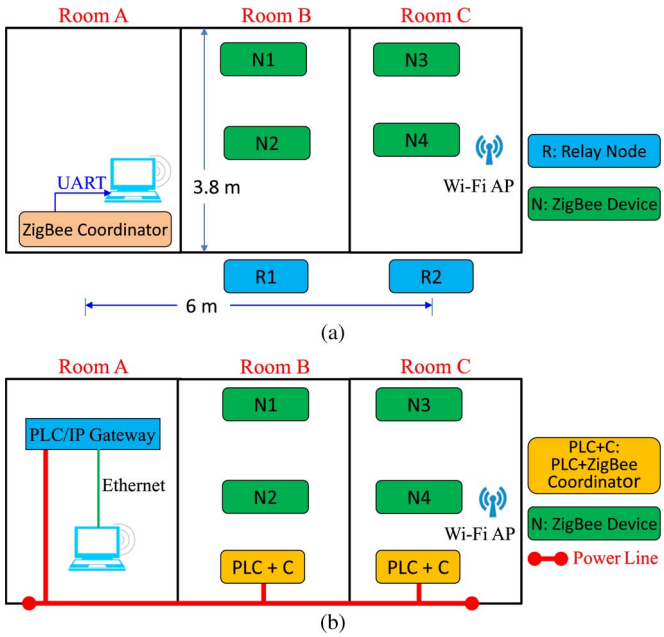

Fig. 2. Architecture of smart home control network based on (a) WSN with relay nodes and (b) WSN plus PLC.

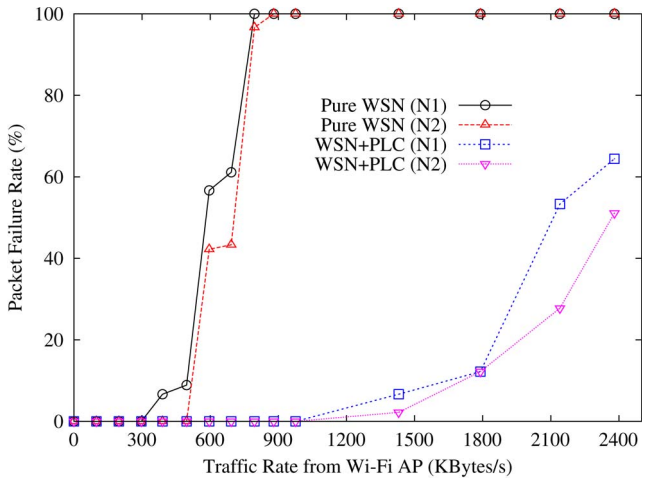

Fig. 3. Performance comparison for end devices N1 and N2 under different network architectures.

which is integrated into the PLC transceiver and is denoted by PLC+C in Fig. 2(b). In other words, the PLC network connects all ZigBee coordinators in different rooms.

Next, the failure rate of packet transmissions in the considered network architectures that are displayed in Fig. 2 is measured. The packet failure rate P_F herein is defined as follows:

$$P_F = \frac{\text{Total number of failed packets}}{\text{Total number of transmitted packets}}. \quad (1)$$

Figs. 3 and 4 show the packet failure rates of individual ZigBee end devices under different network architectures. From Fig. 3, when the ZigBee end device is closer to the WSN relay node or the PLC+C coordinator, the performance is better. That is, the packet failure rate of N2 is smaller than that of N1, as shown in Fig. 3. A similar phenomenon can be found between

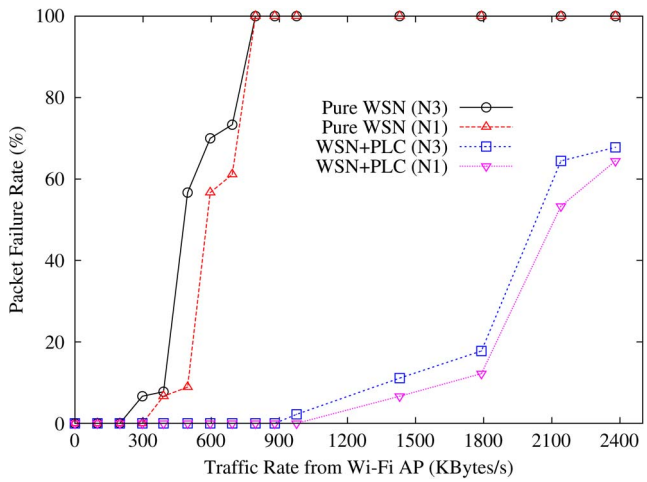

Fig. 4. Performance comparison for end devices N1 and N3 under different network architectures.

end devices N3 and N4. This result is reasonable because a shorter distance yields a better SNR. With respect to wireless interference, when the ZigBee end device is closer to the Wi-Fi AP, it encounters greater interference. Therefore, the packet failure rate of N1 is smaller than that of N3, as shown in Fig. 4. Similar results can be found at N2 and N4.

The results in Figs. 3 and 4 reveal that the performance of the WSN+PLC architecture is much better than that of the pure WSN architecture mainly because, in the pure WSN architecture, the relay nodes still encounter wireless interference from the WLAN. In the WSN+PLC architecture, the WSN signals received by the PLC+C coordinator are transferred to the coordinator in Room A by the PLC network which is immune to wireless interference. Hence, the packet failure rate of the WSN+PLC architecture is much less than that of the pure WSN architecture. On the other hand, compared with the methods in [11], [19], and [20], by modifying the transmission mechanism of WSNs to reduce packet failure rates, no modification in the transmission protocol of WSNs is required when the proposed WSN+PLC architecture is used. Therefore, the proposed WSN+PLC architecture in Fig. 2(b) is a good candidate for the smart home control network.

III. Smart Lighting Control and Energy Saving

A. Smart Control Algorithm for Lighting Systems

To save the most energy, the management system must automatically adjust the working states of home appliances in response to environmental data. The CIE Central Bureau suggests that the minimum illumination (level) of indoor work places should range from 300 to 500 lx [38]. To save energy consumption, natural light must be considered in the design of lighting systems for buildings [31]–[33]. Hence, in the following, a smart control algorithm for lighting systems, as shown in Fig. 5, is proposed.

Fig. 5 shows the workflow of the proposed smart lighting control algorithm that includes the shading control. First, two proper threshold values L and H must be set for the smart control algorithm. For example, the lower threshold L is 500 lx

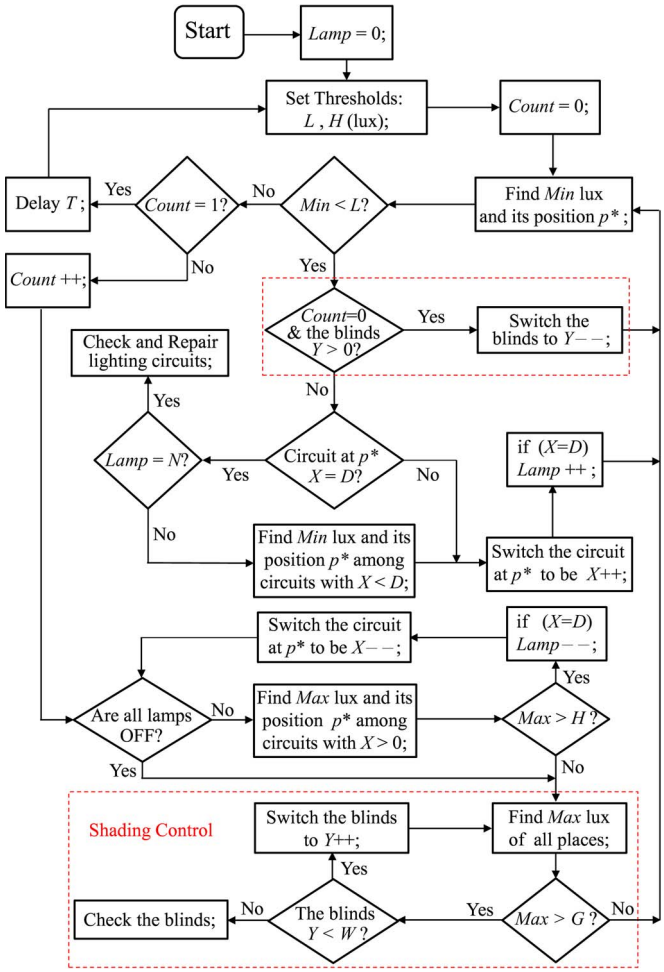

Fig. 5. Proposed smart control algorithm for lighting systems.

[38], and the upper threshold H is 700 lx. Here, the room is assumed to include N lighting circuits, and the illumination by each lighting circuit can be detected by one light sensor. Each lighting circuit provides D levels of digital dimming control [39]. The state of a lighting circuit is denoted by the integer X, where $0 \leq X \leq D$. The state $X = D$ indicates that the lighting circuit is fully ON, and $X = 0$ represents that the lighting circuit is OFF. The window blinds, which are used to prevent glare from the sun, are also assumed to provide a dimming function of W levels. The state of the window blinds is the integer Y, where $0 \leq Y \leq W$. The state $Y = W$ represents that the blinds are fully closed, while $Y = 0$ indicates that the blinds are fully opened.

Subsequently, the algorithm finds the minimum lux Min and its position p^*; if the total illumination (including that by natural light) at p^*, Min, is less than the lower threshold L, then the possibility of using natural light to improve the illumination is first checked (entering the upper shading control blocks in Fig. 5). If $Count = 0$ and the blinds are not fully opened $(Y > 0)$, then the blinds will be switched to the state $Y - 1$; otherwise, increasing the power of the lamps is required. That is, when the total illumination at p^*, Min, is less than the lower threshold L and no more natural light can contribute to the illumination, the state of the lighting circuit at p^* must be checked ($\rightarrow$ "Circuit at p^* $X = D$?") and changed. If the state of the lighting circuit at p^* satisfies $X < D$, then the system will switch the lighting circuit at p^* to the state $X + 1$ ($\rightarrow$ "Switch the circuit at p^* to be $X + +$"). Next, the parameter $Lamp$ will be increased by 1 if $X = D$ ($\rightarrow$ "If $(X = D)$ $Lamp + +$"), and the algorithm will go back to find again the place of the minimum lux ($\rightarrow$ "Find Min lux and its position p^*"). If the state of the lighting circuit at p^* satisfies $X = D$, then the system will try to increase the power of other lighting circuits with $X < D$ ($\rightarrow$ "Find the Min lux and its position p^* among circuits with $X < D$"). This loop continues until $Lamp$ reaches N ($\rightarrow$ "Check and Repair lighting circuits") or the minimum illumination at p^* is not less than L ($\rightarrow$ "$Count = 1$?"). The condition $Lamp = N$ specifies that a lamp may have broken down and must be repaired.

If the illumination levels at all places exceed L, then $Count$ is increased by 1 ($\rightarrow$ "$Count + +$"), and the algorithm proceeds to check whether the illumination at any place with the lighting circuit $X > 0$ is over the upper threshold H ($\rightarrow$ "Find Max lux and its position p^* among circuits with $X > 0$" and "$Max > H$?"); if it does, then the system will decrease the power of the lighting circuit at this location ($\rightarrow$ "Switch the circuit at p^* to be $X - -$") and proceed to find again the place of the maximum illumination ($\rightarrow$ "Find Max lux and its position p^* among circuits with $X > 0$"). This loop continues until the maximum illumination is below H or all lamps are OFF. Next, if the maximum illumination among all places is larger than G, where $G \geq H$, then the blinds must be used to prevent glare from the sun (entering the lower shading control blocks). Finally, the algorithm again returns to the state "Find Min lux and its position p^*." A timer begins immediately after the algorithm enters the state "Delay T." After a prespecified time T, the algorithm restarts.

B. Analysis of Illumination of Fluorescent Lamp

To understand how much energy can be saved using the proposed smart control algorithm, the contribution of the fluorescent lamp to illumination is analyzed first. The analysis of illumination of a fluorescent lamp is based on the following assumptions.

1) The length of a fluorescent lamp is denoted by Γ. Since the length of a fluorescent lamp is usually much larger than the diameter of its tube d such as $\Gamma = 0.59$ m $\gg$ $d = 0.028$ m [40], the fluorescent lamp is treated as a line source of light in the following analysis.
2) Since the light sensors are placed on the working table, the effect of reflection from the floor is ignored. The reflection from walls or obstacles is weaker than the directly incident light, so the scattering effect can also be neglected.

The lamp is assumed to be parallel to the x-axis, and its center is at point $P_0 = (x_0, y_0, z_0)$. Each lamp can be assumed to consist of an infinite number of point light sources. The contribution of the point light source at P_0 to illumination at $P_1 = (x_1, y_1, z_1)$ is denoted by $E_{P_1}(P_0)$, which is given by

$$E_{P_1}(P_0) = \frac{\phi cos\theta}{4\pi R^2} = \frac{\phi}{4\pi R^2} \times \frac{|z_0 - z_1|}{R} \tag{2}$$

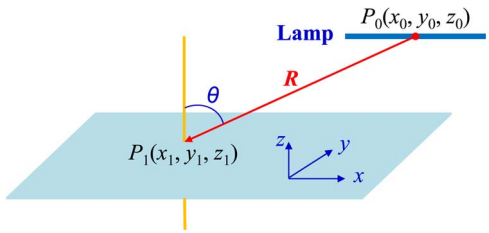

Fig. 6. Illustration of illumination analysis of fluorescent lamp.

where $R = \sqrt{(x_0 - x_1)^2 + (y_0 - y_1)^2 + (z_0 - z_1)^2}$ is the distance between points P_0 and P_1, as shown in Fig. 6. The parameter ϕ is the effective luminous flux by a unit-length (in meter) fluorescent lamp, and it can be computed as follows:

$$\phi = \frac{L_m \times M \times R_f}{\Gamma} \tag{3}$$

where L_m is the total luminous flux by a single fluorescent lamp; M is the lumen maintenance of the fluorescent lamp, and R_f is the lampshade reflection coefficient. The factor $cos\theta$ in (2) represents the contribution of the point light source at P_0 to illumination at P_1 in the z-direction. The total illumination by the fluorescent lamp at point P_1 can be written as follows:

$$E_{P_1}(lamp) = \int_{x_0-\Gamma/2}^{x_0+\Gamma/2} E_{P_1}(x, y_0, z_0)dx. \tag{4}$$

The formula for $E_{P_1}(lamp)$ is derived as follows:

$$E_{P_1}(lamp) = \frac{\phi|z_0 - z_1|}{4\pi\left[(y_0 - y_1)^2 + (z_0 - z_1)^2\right]} \times \left(\frac{x_0 - x_1 + \frac{\Gamma}{2}}{R_1} - \frac{x_0 - x_1 - \frac{\Gamma}{2}}{R_2}\right) \tag{5}$$

where R_1 and R_2 are given by

$$R_1 = \sqrt{\left(x_0 - x_1 + \frac{\Gamma}{2}\right)^2 + (y_0 - y_1)^2 + (z_0 - z_1)^2}, \tag{6}$$

$$R_2 = \sqrt{\left(x_0 - x_1 - \frac{\Gamma}{2}\right)^2 + (y_0 - y_1)^2 + (z_0 - z_1)^2}. \tag{7}$$

Detailed derivations for (5) are given in the Appendix. Table I is the data sheet of the TL-D fluorescent lamps [40]. The reflection coefficient R_f is measured to be 2.16. The listed parameters in Table I are used in the simulations and measurements. The results of an analysis based on (5) are compared with measurements.

Fig. 7 presents the experimental environment for verifying our analytical result in (5). In Fig. 7, the middle points of these four fluorescent lamps are located at coordinates (0, −0.21, 1.84), (0, −0.07, 1.84), (0, 0.07, 1.84), and (0, 0.21, 1.84), respectively. The origin point (0, 0, 0) is on the work surface (xy plane). All units of the x-, y-, and z-axes are in meters. Varying the position of the light meter (HS1010A) enables the

TABLE I
DATA SHEET FOR SET OF FLUORESCENT LAMPS [40]

Number of Lamps in a Set	n	4
Lumen Maintenance 2000h Lumen Maintenance 5000h	M	96% 94%
Luminous Flux	L_m	1275 (lm)
Effective Light-Emitting Length	Γ	589.8 (max) mm
Reflection Coefficient	R_f	2.16

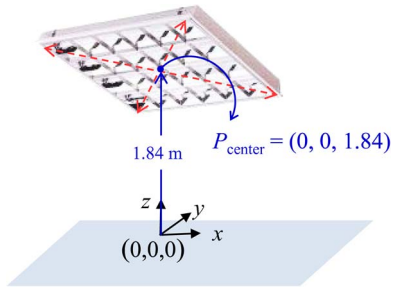

Fig. 7. Environment for verifying the analytical result in (5).

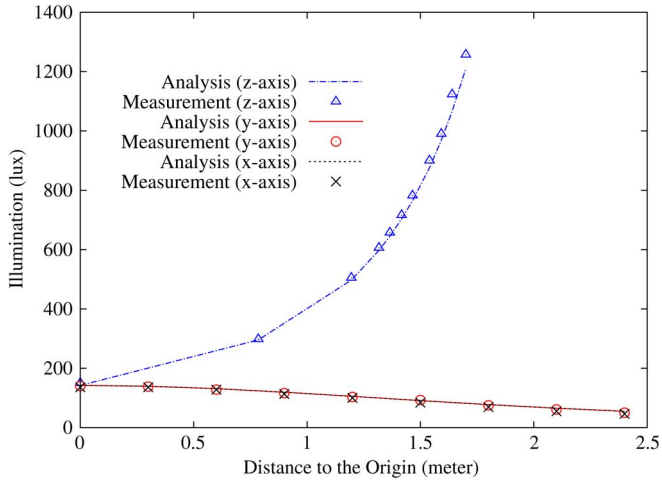

Fig. 8. Illumination levels by a set of lamps at different positions along x-, y-, and z-axes, respectively.

illumination levels at different positions by a set of fluorescent lamps to be obtained. The illumination by only one set of fluorescent lamps was measured in our laboratory at night. Referring to Fig. 7, the illumination in the z-axis was measured along the z-axis at different positions from the middle point of the set of fluorescent lamps below the work surface. Then, on the work surface, the illumination was measured along the x- or y-axis every 0.3 m. The measured results are compared with the results obtained by analysis. Fig. 8 shows the measured illumination levels and the ones determined analytically at different positions along the x-, y-, and z-axes, respectively. From Fig. 8, the difference between the analyzed illumination and the measured illumination is negligible.

In the following, the analytical result in (5) is utilized to simulate illumination by all lamps in a room, and then, the energy saving is evaluated when the proposed smart control algorithm is used with the lighting systems.

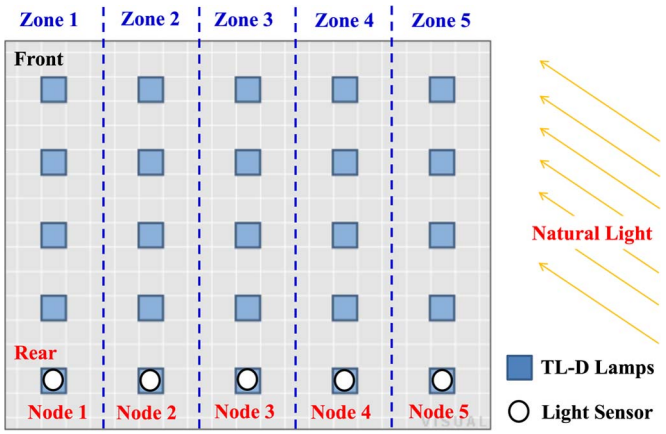

Fig. 9. Layout of lighting system in classroom.

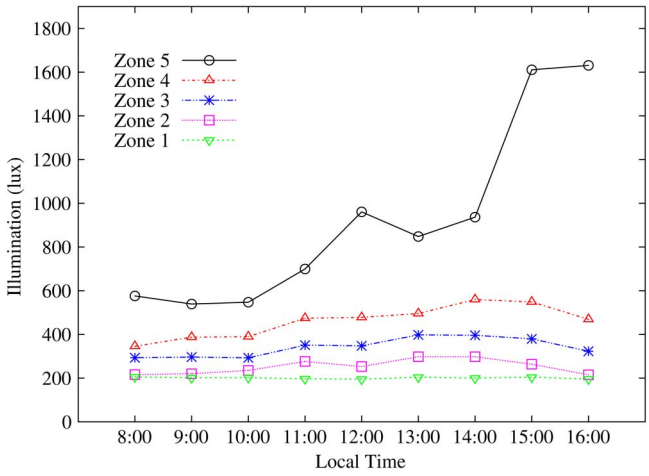

Fig. 10. Illumination of each zone by natural light.

C. Energy Saved by Lighting Using Smart Control

Fig. 9 displays the experimental environment for lighting in the classroom. The sun shines into the classroom from the right. Obviously, the illumination at the right side of the room (Zone 5) will be higher than that at the left side (Zone 1). According to the measurements, the natural light contributes to the illumination levels at the front and the rear of the classroom to slightly different degrees. The average illumination at the rear of the classroom is lower than that at the front of the classroom.

The lighting circuits in a real classroom may not be designed as that in Fig. 9. However, to save power energy consumed by the lighting system, the lighting circuits in Fig. 9 can be reasonably designed as column-based circuits. Hence, Fig. 9 assumes that all lamps in each column belong to the same lighting circuit and can be controlled by an individual switch. Moreover, to demonstrate the superiority of the proposed smart control algorithm, simulations are carried out to evaluate the energy saving of the lighting system in Fig. 9. In our simulations, the analytical result in (5) is used to simulate the illumination by each lamp. However, the background illumination by natural light is measured, as shown in Fig. 10. Notably, to satisfy the minimum illumination requirement at all positions in the classroom, the smart control algorithm uses only the data concerning illumination at the rear of the classroom to control the lighting system. Accordingly, only the illumination data at the rear of the classroom are employed to evaluate performance. Additionally, in the simulations, no shading and dimming control is supported, i.e., $W = 0$ and $D = 1$.

In Fig. 9, the classroom is divided into five zones, and their illumination levels under the smart lighting control are compared. Fig. 10 shows the illumination of each zone by natural light during daytime. According to the measurements, Zone 5 has the strongest illumination because it is the closest to the window on which light is incident. The illumination of Zone 5 by natural light always exceeds 500 lx, so no lighting circuit in Zone 5 needs to be turned on based on the smart control algorithm in Fig. 5. However, the lighting circuits in the other zones must be turned on to meet the minimum illumination requirement of 500 lx.

Using the analytical result in (5) and the measured data in Fig. 10, the illumination of the classroom in Fig. 9 under the smart lighting control is simulated. Since the proposed algorithm is heuristic, the result of the optimal solution that can minimize the power consumption of lighting systems and satisfy the minimum illumination requirement is also included. Fig. 11 shows the simulated illumination levels of Zones 1, 3, and 5, respectively, under the proposed smart control scheme and the scheme without smart control (all lamps ON). In Fig. 11, one average sample per hour is plotted from all simulated illumination data points, and the contribution to illumination by natural light is also included. In the proposed smart control scheme, the minimum illumination requirement L (lower threshold) is set to 500 lx, and the upper threshold H equals 700 lx.

With reference to Fig. 11(a), the illumination of Zone 1 under the proposed smart control scheme is close to that when all lamps are ON. This is because Zone 1 is the farthest from the window on which light is incident, so natural light contributes less to the illumination of Zone 1 than to that of any other zone. Thus, almost all the time, the lamps in Zone 1 must be turned on under the smart control. Accordingly, no significant difference exists between the smart control scheme and the one with all lamps ON. Referring to Fig. 11(a) and (b), the illumination of Zone 3 is always larger than that of Zone 1 when all lamps are ON. However, the illumination of Zone 3 remains almost the same as that of Zone 1 under the smart control, illustrating that only sometimes are the lamps at Zone 3 turned on under the smart control.

Zone 5 is the nearest area to the window on which light is incident, so the natural light contributes more to the illumination of Zone 5 than to that of any other zone. Therefore, the lamps in Zone 5 rarely have to be turned on under the proposed smart control scheme. Accordingly, the illumination under the proposed smart control scheme is much less than that when all lamps are ON, as shown in Fig. 11(c). To show how much energy can be saved under the smart control, the absolute value of the total power consumed by lighting in the classroom is depicted in Fig. 12. The gap between the curves of the smart control scheme and that with all lamps ON represents the energy saving that can be achieved using

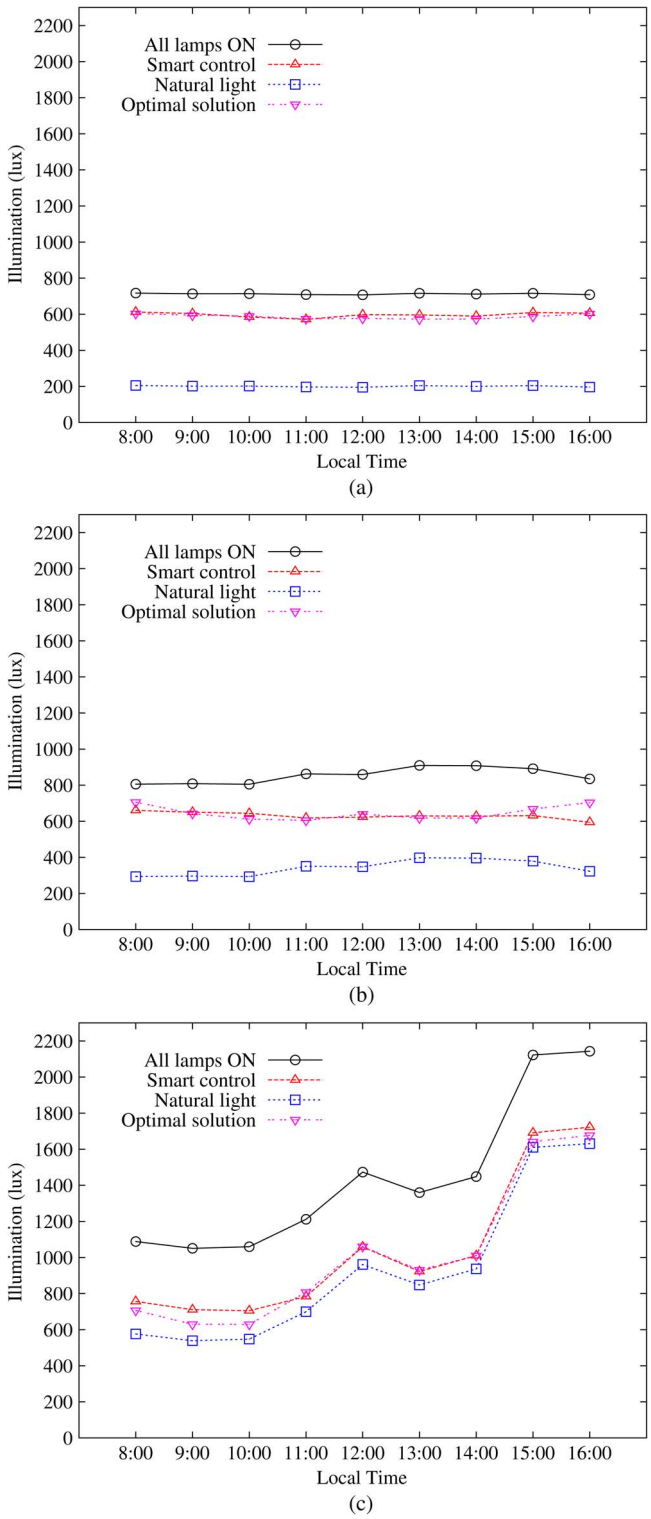

Fig. 11. Illumination of (a) Zone 1, (b) Zone 3, and (c) Zone 5.

the smart control mechanism. The simulation results demonstrate that the proposed smart lighting control scheme provides significant energy saving. Moreover, the performance of the proposed smart control algorithm is almost coincident with that of the optimal solution, indicating that the proposed heuristic algorithm is near optimal.

Next, define the energy saving ratio as follows. The energy saving ratio S is defined as the percentage of power consumption that can be saved when the smart control scheme is employed, relative to the situation in which all lamps are ON. It is computed using the following equation:

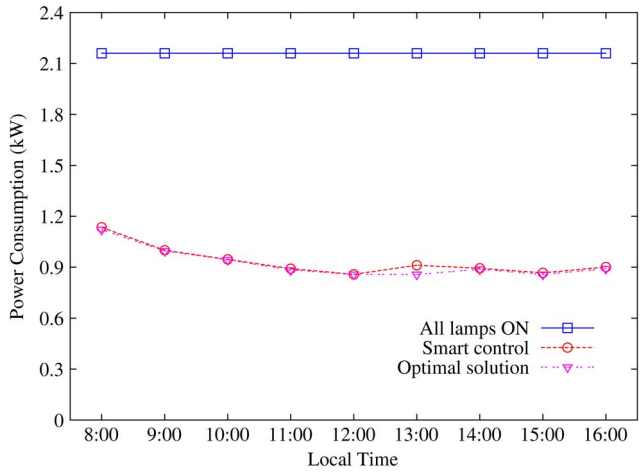

Fig. 12. Absolute value of power consumed by lighting in the classroom.

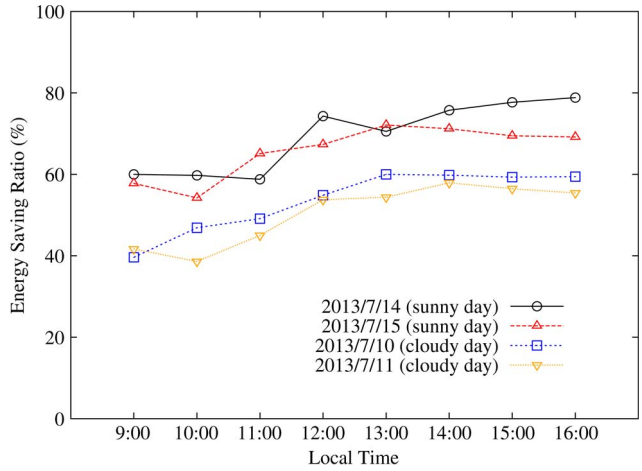

Fig. 13. Energy saving ratios on sunny and cloudy days.

$$S = \left(1 - \frac{\alpha}{\beta}\right) \times 100\% \tag{8}$$

where α is the number of lamps that are turned on under the smart control scheme and β represents the total number of lamps.

To clearly demonstrate the superiority of our proposed smart control scheme, the energy saving ratio is studied by simulation. Fig. 13 shows the energy saving ratios under the proposed smart control scheme on sunny and cloudy days. According to the simulation results, the energy saved on a sunny day is larger than that saved on a cloudy day. Even on cloudy days, the proposed smart control scheme reduces the energy consumed by lighting in the classroom by at least 40%, indicating that the proposed smart control mechanism is excellent.

In Figs. 11–13, the packet failure rate of the sensed illumination data is assumed to be zero. However, packet error or loss is inevitable in a real environment. To counteract the packet loss problem, the proposed smart lighting control algorithm is designed as follows. Whenever a packet loss occurs, the

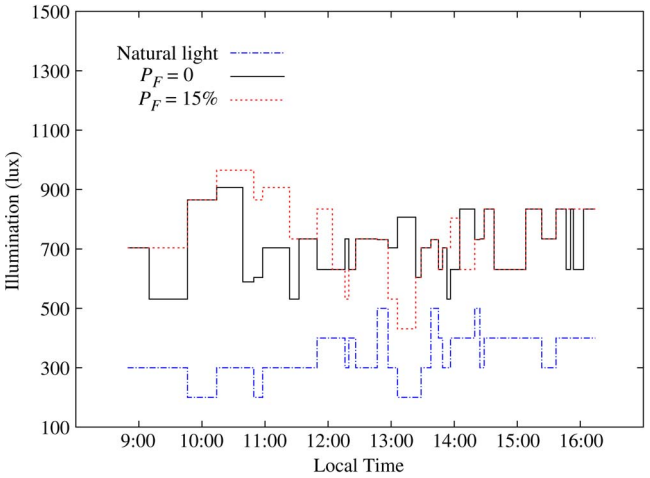

Fig. 14. Impact of packet failure rate on the performance of smart lighting control (natural light on 2013/7/11).

lighting control algorithm must defer making a decision until new environmental data from all sensor nodes arrive correctly. That is, no decision can be made and the states of all lamps remain unchanged when any packet is lost. To study the impact of packet failure rate on the performance of the proposed smart lighting control, the illumination levels of Zone 3 under the scenarios with $(P_F = 15\%)$ and without $(P_F = 0)$ packet failure are compared in Fig. 14 by simulation. The simulation environment is similar to that of Figs. 11–13 except that the illumination data loss event is simulated. Moreover, one instantaneous sample per 5 min is extracted and plotted from all simulated illumination data points. According to Fig. 14, packet loss in WSNs may lead to misses of tuning off lamps for saving power or turning on lamps for satisfying the minimum illumination requirement of 500 lx. Therefore, constructing a reliable data gathering and communication network such as the proposed WSN+PLC for the home automation control system is extremely required.

IV. Implementation of Prototype of Proposed Smart Home Control Network

A. System Block Diagram

The block diagram of the smart home control system is composed of three parts—data collection, communication, and appliance control, as shown in Fig. 15. Data collection is realized using WSNs. The information thus obtained is sent by the WSN and relayed by the PLC and the IP network to the management station. After the environmental information is received, the management station determines the states of all home appliances to optimize the power consumption. Subsequently, the management station sends control commands to renew the states of all home appliances via the PLC.

The proposed architecture, described earlier, simplifies the optimization problem of node placement in WSNs and mitigates the impact of wireless interference. Furthermore, the PLC/IP gateway, which connects the PLC and the IP networks, enables Internet access for the remote monitoring of the smart home network and the control of it in real time.

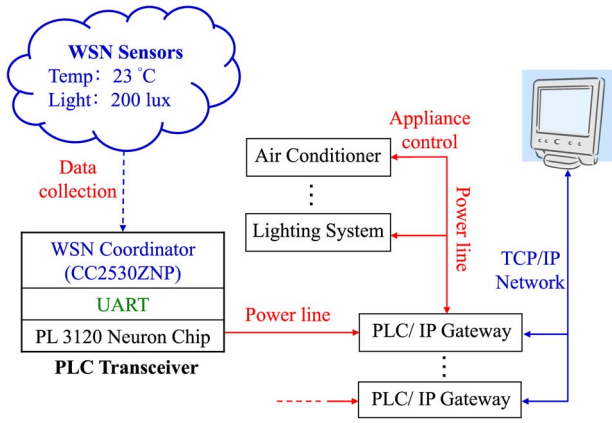

Fig. 15. System block diagram.

Additionally, the proposed architecture is highly scalable since several PLC/IP gateways can be connected to the management station to extend the smart home control network, as shown in Fig. 15. The major tasks in constructing the proposed smart home control system include integrating the WSN coordinator with the PLC transceiver and integrating each home appliance switch with the PLC transceiver. Related electronic components that are required in constructing a smart home control network are described in subsequent sections.

B. PL 3120 Smart Transceiver

To counteract the impact of background noise in PLCs, the PL 3120 chip [23] is used as the PLC module herein. The PL 3120 smart transceiver is used for the following reasons. First, the PL 3120 smart transceiver uses narrow-band signaling and thus has the ability to communicate across transformers. This transceiver employs a dual-carrier frequency signaling technology and can automatically switch to the secondary communication frequency whenever the primary frequency is blocked by noise. In the worst case, the PL 3120 smart transceiver can retransmit data up to three times to ensure that the data are received correctly. Second, the PL 3120 smart transceiver uses a variant of the p-persistent CSMA medium access control (MAC) protocol that is called the predictive p-persistent CSMA. Unlike the original CSMA, the predictive p-persistent CSMA protocol is dedicated to network control applications and generally operates on short data packets under bursty traffic conditions. When the network is idle, all devices can transmit randomly over a minimum 16-slot period, which is called the randomizing window. As the network load increases, the randomizing window increases by a factor of a, where a ranges from 1 to 63.

The PL 3120 transceiver uses a wide power supply range (+8.5 to +18 Vdc) and supports very low receive mode current consumption. Additionally, if, during transmission, the power supply voltage falls to a level that is insufficient to ensure reliable signaling, the transceiver stops transmitting until the power supply voltage rises to an acceptable level. These features allow the use of a power supply with a smaller current capacity required, yielding a reduction in the size, cost, and thermal dissipation of the power supply. However, since the input of

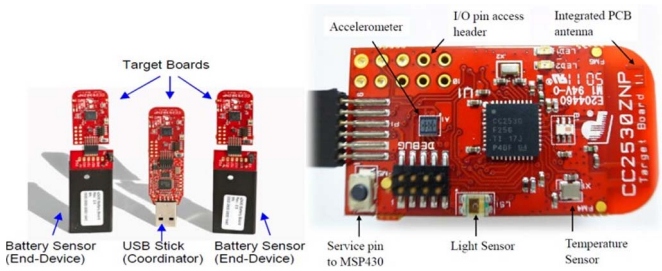

Fig. 16. CC2530 ZigBee devices (from Texas Instruments SWRU268A).

the power supply is connected directly to the communication channel, a power supply may attenuate the communication signal and couple noise into the PLC transceiver. To preserve the full communication capability of the PLC transceiver, it is important to ensure that the power supply does not impair communication performance. Several "preverified" power supply options given in the data book of PL 3120 [23] can be considered. The power consumption of the used PLC module in this work is less than 7.5 W.

To control home appliances via the PLC, each home appliance switch must be integrated with a PLC transceiver. The PL 3120 transceiver provides twelve I/O pins which can be configured to operate in one or more of the 38 predefined standard input/output modes [23]. Hence, there is no difficulty to enable it to interface with application circuits and home appliance switches using a small number of inexpensive components such as resistors and capacitors.

C. CC2530 ZigBee Devices

In this paper, the CC2530 ZigBee network processor (ZNP) [41], displayed in Fig. 16, is used to collect environmental information. CC2530ZNP supports several sensors, such as temperature, light, and motion sensors. The target board that is connected to the USB stick can be programmed with a coordinator sample application to become a WSN coordinator. The coordinator can set up the entire WSN network and configure related parameters.

Each isolated WSN system can have a single coordinator. The coordinator initially sets the beacon signals to coordinate all nodes in the WSN. If the end device cannot receive or recognize the beacon signals, then it asks the coordinator to try again. After the end device has successfully communicated with the coordinator, it stays awake and sends data in a manner determined by the timer. The state of the system then switches between idle and transmission until the end device loses contact with the coordinator.

D. Integration of PLC and WSN

In the CC2530 ZigBee device, the microcontroller MSP430F2274 is mainly used to control the ZigBee device and related data communications among sensors, CC2530ZNP, and the USB stick. The ZigBee device provides a serial communication interface for data communications between the CC2530ZNP and the MSP430F2274 microcontroller. Therefore, the PLC transceiver can directly fetch environmental

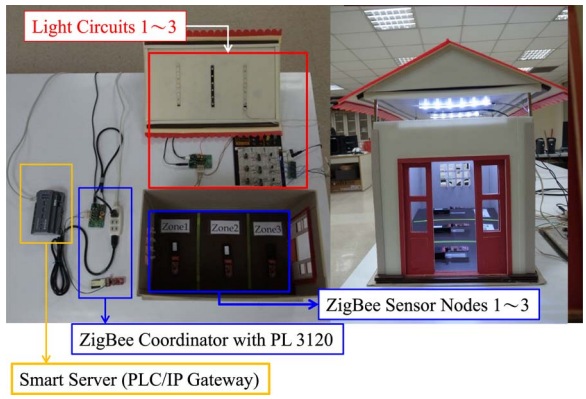

Fig. 17. Prototype of proposed smart home control network.

data from the appropriate I/O pins, such as pin 34 (Tx) and pin 35 (Rx), of the CC2530ZNP. To achieve this goal, an interface between the PLC transceiver and the ZigBee coordinator for direct communication is designed. Our approach is described as follows. First, different programs for controlling data communications are written into the PLC transceiver and the ZigBee coordinator, respectively. Next, the USB stick is removed from the ZigBee coordinator. Finally, the PLC transceiver and the ZigBee coordinator are connected to achieve one-way data transmissions between them. Such a method simplifies the design of an environmental data gathering system. However, there is no difficulty to implement a two-way transmission between the WSN coordinator and the PLC transceiver if other designs require doing so.

E. System Prototype

To demonstrate the feasibility of the proposed system architecture, a prototype is constructed, as shown in Fig. 17. The prototype consists of the ZigBee WSN, the PLC network, and the PLC/IP gateway (smart server) whose power consumption is less than 15 W. Since home appliances must be connected to power lines, the management station can control and monitor the states of home appliances via the PLC/IP gateway. Therefore, using a PLC network as the backbone is a convenient way to realize a smart home control network. In the prototype, the ZigBee WSN is employed only to collect the environmental parameters, such as temperature and illumination. The sensor nodes detect these parameters and send them to the ZigBee coordinator via the WSN. Finally, these parameters are transferred to the management system via the PLC and the IP networks.

Several experiments on the prototype system are conducted. First, the prototype system, which adopts the smart control algorithm that is presented in Fig. 5, is applied to the model house in Fig. 17. In the prototype system, no shading and dimming control is supported. Fig. 18 shows the developed monitoring application graphical user interface. The lower and the upper thresholds in the smart control algorithm are set to 500 and 700 lx, respectively. Initially, all three LED strip lamps in the model house are in the OFF state. According to the experimental results in Fig. 18, the lighting system takes approximately 10 s to become stable (at 18:58:17) after the test starts (at 18:58:07). All experimental tests show that the

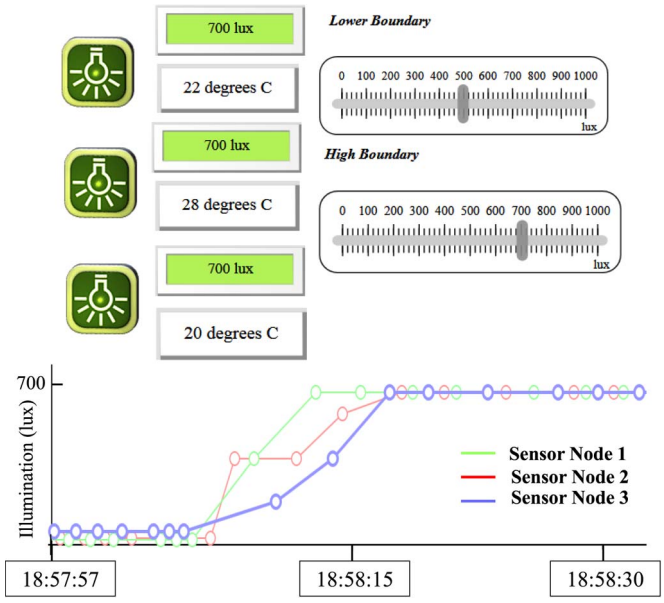

Fig. 18. Web page for monitoring proposed lighting control system.

prototype system works well and controls the LED lamps based on the measured illumination in the model house. Notably, the transition time to reach the control goal depends on the transmission period of ZigBee sensor nodes. A smaller transmission period can achieve a shorter transition time to reach the control goal. However, the battery lifetime of a sensor node decreases as the transmission period reduces. In our experiments, the transmission period of each sensor node is set to 3 s. Another way to shorten the transition time is to use the analysis result (5) in the smart control algorithm. When (5) is used, the smart control algorithm can automatically update the illumination and determine the states of all lamps quickly without resorting to several rounds of illumination gathering. However, the model of the lamps must be known first, and the sensor nodes must be fixed. Additionally, the aging of lamps may also lead to an estimation error of illumination.

Subsequently, the experimental environment is changed from the model house to the classroom. In the classroom, the lighting system includes three lighting circuits, Circuits 1 to 3. Each lighting circuit consists of a column of lamps and is controlled by an independent switch. Circuits 1 and 3 are the farthest and the nearest to the windows, respectively. Three sensor nodes are equally spaced in the classroom to detect the illumination levels of locations near the windows and that far away from them.

Fig. 19(a) shows the results of an experiment about the operation of the proposed smart lighting control algorithm on a rainy day. According to the results, the system may oscillate and need a transition period to become stable. Initially, all circuits are in the OFF state. Thus, the illumination at each sensor node is below L (500 lx). Accordingly, the smart control algorithm immediately turns on Circuit 1. A similar process is performed for Circuit 2. Since the illumination of Node 3 is still less than 500 lx, Circuit 3 is also turned on at $t = 9$ s after the experiment starts. Thus, the illumination levels at all nodes exceed L. However, the illumination at Node 3 now exceeds H (700 lx), so the system turns off Circuit 3, causing

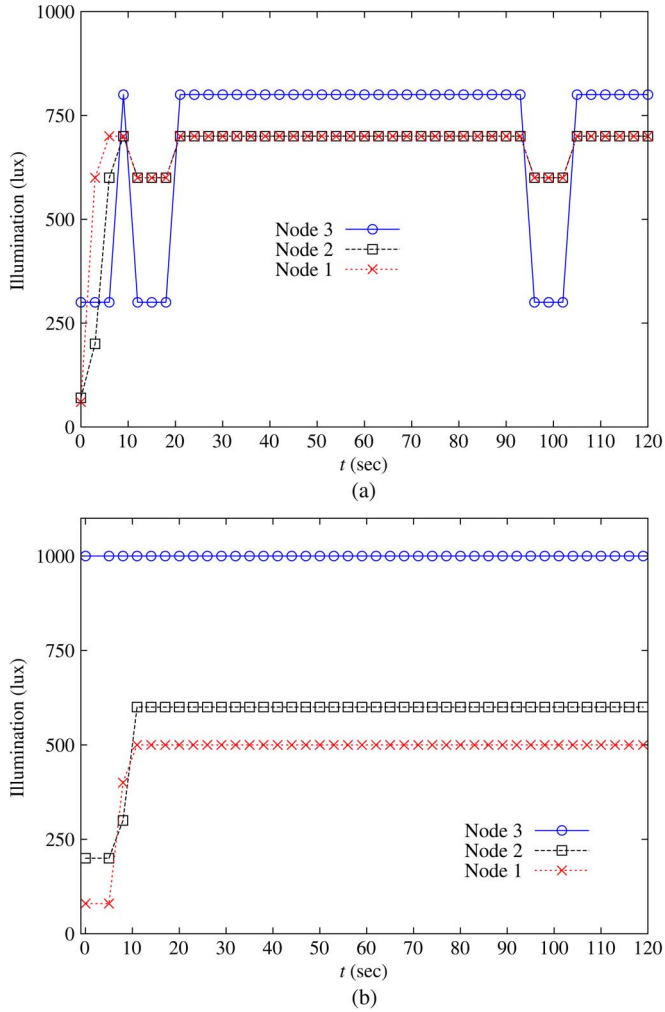

Fig. 19. Experimental results concerning proposed smart lighting control algorithm on a (a) rainy day and a (b) cloudy day.

the illumination at Node 3 to fall to below 500 lx. The smart control algorithm in Fig. 5 returns to the state "Find Min lux and its position p^*" to ensure that the illumination levels at all nodes meet the minimum illumination requirement. Therefore, Circuit 3 is turned on, and the illumination at Node 3 is larger than H again. Since the parameter $Count$ equals 1 at this moment, the smart control algorithm enters the state "Delay T." Now, all circuits are ON, and the lighting system is stable. Since the parameter T is set to 60 s in this experiment, the algorithm leaves the state "Delay T" and restarts the procedure after about 60 s. To effectively eliminate the oscillation phenomenon and save more energy, the lighting system must support the dimming function. If the lighting system does not support the dimming function, then a longer delay T such as 10 min can be considered, or the hysteresis condition $Max > L + \Delta$, where Δ is the illumination contribution by a lighting circuit, can be added into the proposed smart lighting control algorithm to avoid the oscillation phenomenon.

Another experiment is conducted at the same classroom on a cloudy day. Fig. 19(b) displays the experimental results. Initially, all circuits are in the OFF state, and the illumination levels at Nodes 1 and 2 are below L (500 lx) while that of Node 3 is over H (700 lx). Hence, according to the smart control

TABLE II
COMMUNICATION PERFORMANCE

Total Number of Packets Transmitted		1061
Packet Reliability	Number of Success	1052
	Packet Failure Rate P_F	0.8%
End-to-End Packet Delay	Minimum	46 ms
	Maximum	135 ms
	Average	75 ms
	Standard Deviation	16 ms

algorithm, only Circuits 1 and 2 are turned on. If Circuit 3 is turned on, the illumination of Node 3 reaches about 1500 lx. Obviously, turning on Circuit 3 wastes energy and increases the tiredness felt in people's eyes. Therefore, a smart control system must ensure that the illumination levels at all positions exceed the minimum requirement while saving energy. All experiments conducted earlier demonstrate that both the prototype system and the proposed smart control algorithm work correctly and perform well, no matter what the weather is.

To understand the communication performance of the prototype system, the packet delay and reliability are also measured. Three sensor nodes are evenly spaced in our laboratory, and the PLC+C coordinator is located at the center of our laboratory. Each sensor node transmits one packet every 3 s, and the payload of each packet only includes the sequence number and illumination information. Packets are originated by sensor nodes and then traverse the WSN link, the power line, and the IP network to the management station. To measure the end-to-end packet delay, one sensor node is connected to a PC via the USB port to capture the sending time of a packet. Packets from the other two sensor nodes can be viewed as the background traffic for contention. Packets finally arrive at the management station, and their arrival times can be recorded. Subsequently, the packet delay and reliability can be evaluated. Before the measurement, the clocks of the PC and the management station must be synchronized using the Network Time Protocol program or the IEEE 1588 Precision Time Protocol. Table II shows the measurement results. According to Table II, the packet failure rate is about 0.8%, and the average end-to-end packet delay is about 75 ms. Since the packet is short and the network propagation delay is usually less than a microsecond in a smart home environment, the packet delay is mainly incurred by the MAC protocols of the WSN and the PLC.

V. CONCLUSION

This paper has designed a novel network architecture and a smart lighting control algorithm for smart homes. The proposed smart home control network employs the PLC as the network backbone and the WSN for data sensing. The proposed network infrastructure possesses the advantages of both WSNs and PLCs. It simplifies the problem of setting up relay nodes in WSNs and mitigates the impact of wireless interference. It is also highly scalable and can be applied to intelligent buildings. A prototype of the proposed smart home control network with the smart lighting control was implemented. Simulations and practical experiments were conducted to demonstrate that the implemented prototype system works well and that the proposed smart home control network provides an outstanding packet failure rate and considerable energy saving. Although numerical results have shown that the energy saving ratio in lighting is good, control of other home appliances, such as HVAC&R, must also be considered in future work to save more electrical energy.

To fulfill the proposed solution in existing homes or buildings, some installation costs may be induced. For example, the cost of a digital switch with the PLC module is about several tens of U.S. dollars. As to the cost of a ZigBee device, it may be down to several U.S. dollars. The most expensive equipment in the proposed solution is the smart server (PLC/IP gateway) which costs about several hundreds of U.S. dollars. However, since a smart server can manage up to hundreds of devices, it is enough to use only one smart server for controlling lighting systems and home appliances in a home or a small building. Therefore, compared with the cost saving on electricity in the long term, the induced installation cost in the proposed solution is relatively low.

APPENDIX
ANALYSIS OF ILLUMINATION OF FLUORESCENT LAMP

According to (2), the illumination by the fluorescent lamp is rewritten as follows:

$$E_{P_1}(lamp) = \frac{\phi|z_0 - z_1|}{4\pi} \times \int_{x_0-\Gamma/2}^{x_0+\Gamma/2} \left[(x-x_1)^2 + (y_0-y_1)^2 + (z_0-z_1)^2\right]^{-\frac{3}{2}} dx. \quad (9)$$

Changing variables $u = x - x_1$, $A = y_0 - y_1$, $B = z_0 - z_1$, and $C = \phi|z_0 - z_1|/4\pi$ yields the illumination by the fluorescent lamp as

$$E_{P_1}(lamp) = C \int_{x_0-x_1-\Gamma/2}^{x_0-x_1+\Gamma/2} (u^2 + A^2 + B^2)^{-\frac{3}{2}} du. \quad (10)$$

Next, considering the case that $x_0 - x_1 - \Gamma/2 \geq 0$ and $x_0 - x_1 + \Gamma/2 \geq 0$, let $u = \sqrt{(A^2+B^2)/(v^2-1)}$, $v_0 = \sqrt{1 + ((A^2+B^2)/(x_0 - x_1 - \Gamma/2)^2)}$, and $v_1 = \sqrt{1 + ((A^2+B^2)/((x_0 - x_1 + \Gamma/2)^2)}$; the definite integral in (10) can now be rearranged as follows:

$$\begin{aligned} E_{P_1}(lamp) &= -C \int_{v_0}^{v_1} \left[\frac{(A^2+B^2)v^2}{v^2-1}\right]^{-\frac{3}{2}} \frac{v\sqrt{A^2+B^2}}{\sqrt[3]{v^2-1}} dv \\ &= \frac{-C}{A^2+B^2} \int_{v_0}^{v_1} v^{-2} dv \\ &= \frac{C}{A^2+B^2}\left(\frac{1}{v_1} - \frac{1}{v_0}\right). \end{aligned} \quad (11)$$

Because $(u^2 + A^2 + B^2)^{-(3/2)}$ in (10) is an even function of u, for the case that $x_0 - x_1 - \Gamma/2 < 0$ and $x_0 - x_1 + \Gamma/2 < 0$, one can show that

$$E_{P_1}(lamp) = \frac{C}{A^2 + B^2}\left(\frac{1}{v_0} - \frac{1}{v_1}\right). \quad (12)$$

For the case that $x_0 - x_1 - \Gamma/2 < 0$ and $x_0 - x_1 + \Gamma/2 \geq 0$, one can show that

$$E_{P_1}(lamp) = \frac{C}{A^2 + B^2}\left(\frac{1}{v_0} + \frac{1}{v_1}\right). \quad (13)$$

Finally, substituting the parameters A, B, C, v_0, and v_1 into (11)–(13) yields (5) no matter what the values of $x_0 - x_1 - \Gamma/2$ and $x_0 - x_1 + \Gamma/2$ are.

Acknowledgment

The authors would like to thank their colleagues, Prof. S.-Y. Lin and Prof. W.-L. Chen, and the anonymous reviewers, for their valuable comments and suggestions that have significantly improved the quality of this paper.

References

[1] R. Missaoui, H. Joumaa, S. Ploix, and S. Bacha, "Managing energy smart homes according to energy prices: Analysis of a building energy management system," *Energy Buildings*, vol. 71, pp. 155–167, Mar. 2014.
[2] C. Molitor *et al.*, "Multiphysics test bed for renewable energy systems in smart homes," *IEEE Trans. Ind. Electron.*, vol. 60, no. 3, pp. 1235–1248, Mar. 2013.
[3] D. M. Han and J. H. Lim, "Smart home energy management system using IEEE 802.15.4 and Zigbee," *IEEE Trans. Consum. Electron.*, vol. 56, no. 3, pp. 1403–1410, Aug. 2010.
[4] C. Suh and Y.-B. Ko, "Design and implementation of intelligent home control systems based on active sensor networks," *IEEE Trans. Consum. Electron.*, vol. 54, no. 3, pp. 1177–1184, Aug. 2008.
[5] J. Byun, B. Jeon, J. Noh, Y. Kim, and S. Park, "An intelligent self-adjusting sensor for smart home services based on ZigBee communications," *IEEE Trans. Consum. Electron.*, vol. 58, no. 3, pp. 794–802, Aug. 2012.
[6] H. Wang and J. Wang, "Design and implementation of a smart home based on WSN and AMR," *Appl. Mech. Mater.*, vol. 271-272, pp. 1485–1489, 2013.
[7] J. M. Wang and H. B. Wei, "Design of smart home management system based on GSM and Zigbee," *Adv. Mater. Res.*, vol. 842, pp. 703–707, 2014.
[8] K. Gill, S. H. Yang, F. Yao, and X. Lu, "A ZigBee-based home automation system," *IEEE Trans. Consum. Electron.*, vol. 55, no. 2, pp. 422–430, May 2009.
[9] W. Liu and Y. Yan, "Application of ZigBee wireless sensor network in smart home system," *Int. J. Advancements Comput. Technol.*, vol. 3, no. 5, pp. 154–160, Jun. 2011.
[10] V. C. Gungor, B. Lu, and G. P. Hancke, "Opportunities and challenges of wireless sensor networks in smart grid," *IEEE Trans. Ind. Electron.*, vol. 57, no. 10, pp. 3557–3564, Oct. 2010.
[11] X. Cao, J. Chen, Y. Xiao, and Y. Sun, "Building-environment control with wireless sensor and actuator networks: Centralized versus distributed," *IEEE Trans. Ind. Electron.*, vol. 57, no. 11, pp. 3596–3605, Nov. 2010.
[12] M. Magno *et al.*, "Extended wireless monitoring through intelligent hybrid energy supply," *IEEE Trans. Ind. Electron.*, vol. 61, no. 4, pp. 1871–1881, Apr. 2014.
[13] S. D. T. Kelly, N. K. Suryadevara, and S. C. Mukhopadhyay, "Towards the implementation of IoT for environmental condition monitoring in homes," *IEEE Sensors J.*, vol. 13, no. 10, pp. 3846–3853, Oct. 2013.
[14] D. Dietrich, D. Bruckner, G. Zucker, and P. Palensky, "Communication and computation in buildings: A short introduction and overview," *IEEE Trans. Ind. Electron.*, vol. 57, no. 11, pp. 3577–3584, Nov. 2010.
[15] R. Kavitha, G. M. Nasira, and N. Nachamai, "Smart home systems using wireless sensor network—A comparative analysis," *Int. J. Comput. Eng. Technol.*, vol. 3, no. 3, pp. 94–103, 2012.
[16] J. Li, L. H. Andrew, C. H. Foh, M. Zukerman, and H. H. Chen, "Connectivity, coverage and placement in wireless sensor networks," *Sensors*, vol. 9, no. 10, pp. 7664–7693, 2009.
[17] D. Yang, Y. Xu, and M. Gidlund, "Wireless coexistence between IEEE 802.11- and IEEE 802.15.4-based networks: A survey," *Int. J. Distrib. Sensor Netw.*, vol. 2011, no. 2011, 2011, Art. ID. 912152.
[18] L. Angrisani, M. Bertocco, D. Fortin, and A. Sona, "Experimental study of coexistence issues between IEEE 802.11b and IEEE 802.15.4 wireless networks," *IEEE Trans. Instrum. Meas.*, vol. 57, no. 8, pp. 1514–1523, Aug. 2008.
[19] L. Tytgat, O. Yaron, S. Pollin, I. Moerman, and P. Demeester, "Analysis and experimental verification of frequency-based interference avoidance mechanisms in IEEE 802.15.4," *IEEE/ACM Trans. Netw.*, vol. 23, no. 2, pp. 369–382, Apr. 2015.
[20] X. Zhang and K. G. Shin, "Gap Sense: Lightweight coordination of heterogeneous wireless devices," in *Proc. IEEE INFOCOM*, Apr. 2013, pp. 3094–3101.
[21] Website of X10. [Online]. Available: http://www.x10.com/
[22] EIA Home Automation System (CEBus) Interim Standard IS-60 1992
[23] Website of Echelon. [Online]. Available: http://www.echelon.com/
[24] Website of HomePlug Alliance, Resources & White Papers/HomePlug AV White Paper 2013. [Online]. Available: http://www.homeplug.org/home/
[25] A. A. Amarsingh, H. A. Latchman, and D. Yang, "Narrowband power line communications: Enabling the smart grid," *IEEE Potentials Mag.*, vol. 33, no. 1, pp. 16–21, Jan./Feb. 2014.
[26] Y. J. Lin, H. A. Latchman, M. Lee, and S. Katar, "A power line communication network infrastructure for the smart home," *IEEE Trans. Wireless Commun.*, vol. 9, no. 6, pp. 104–111, Dec. 2002.
[27] V. Degardin, K. Kilani, L. Kone, M. Lienard, and P. Degauque, "Feasibility of a high bit rate power line communication between an inverter and a motor," *IEEE Trans. Ind. Electron.*, vol. 61, no. 9, pp. 4816–4823, Sep. 2014.
[28] A. Al-Mulla and A. Elsherbini, "Demand management through centralized control system using power line communication for existing buildings," *Energy Convers. Manag.*, vol. 79, pp. 477–486, Mar. 2014.
[29] L. J. Qin, Z. Z. Shen, and F. Jiao, "Intelligent streetlight energy-saving system based on LonWorks power line communication technology," in *Proc. Int. Conf. Elect. Utility DRPT*, Jul. 2011, pp. 663–667.
[30] INSTEON Technology, v. 2.0, 2005–2013 Whitepaper: The details. [Online]. Available: http://www.insteon.net/pdf/insteondetails.pdf, v. 2.0, 2005–2013
[31] P. Ihm, A. Nemri, and M. Krarti, "Estimation of lighting energy savings from daylighting," *Building Environ.*, vol. 44, no. 3, pp. 509–514, Mar. 2009.
[32] B. Sun *et al.*, "Building energy management: Integrated control of active and passive heating, cooling, lighting, shading, ventilation systems," *IEEE Trans. Autom. Sci. Eng.*, vol. 10, no. 3, pp. 588–602, Jul. 2013.
[33] G. Parise and L. Martirano, "Daylight impact on energy performance of internal lighting," *IEEE Trans. Ind. Appl.*, vol. 49, no. 1, pp. 242–249, Jan./Feb. 2013.
[34] I. A. Zualkernan, A. R. Al-Ali, M. A. Jabbar, I. Zabalawi, and A. Wasfy, "InfoPods: Zigbee-based remote information monitoring devices for smart-homes," *IEEE Trans. Consum. Electron.*, vol. 55, no. 3, pp. 1221–1226, Aug. 2009.
[35] Y. Lin, R. Kong, R. She, and S. Deng, "Design and implementation of remote/short-range smart home monitoring system based on ZigBee and STM32," *Res. J. Appl. Sci., Eng. Technol.*, vol. 5, no. 9, pp. 2792–2798, Jan. 2013.
[36] J. Hu and W. Zhang, "Design of remote intelligent home system based on ZigBee and GPRS technology," in *Proc. 2nd Int. Conf. CECNet*, Apr. 2012, pp. 264–267.
[37] G. J. Kim, C. S. Jang, C. H. Yoon, S. J. Jang, and J. W. Lee, "The implementation of smart home system based on 3G and ZigBee in wireless network systems," *Int. J. Smart Home*, vol. 7, no. 3, pp. 311–320, May 2013.
[38] *Lighting of Indoor Work Places*, ISO 8995-1:2002(E), May 2002, 1st Edition.
[39] C.-A. Cheng, H.-L. Cheng, K.-J. Lin, E.-C. Chang, and C.-H. Yen, "Implementation of a digitally dimming controlled lighting system for two-area fluorescent lamps," in *Proc. 5th ICIEA*, Jun. 15–17, 2010, pp. 2281–2286.
[40] Philips TL-D LIFEMAX Super 80 18w/865 Fluorescent Lamp. [Online]. Available: http://www.ecat.lighting.philips.com/
[41] *A True System-on-Chip Solution for 2.4-GHz IEEE 802.15.4 and ZigBee Applications (Rev. B)*, CC2530 Datasheet, Feb. 2011.

Mingfu Li received the B.S. and Ph.D. degrees in electrical engineering from National Taiwan University, Taipei, Taiwan, in 1991 and 1998, respectively.

From 1998 to 2003, he worked as an Associate Researcher in the Telecommunication Laboratories at Chunghwa Telecom Company, Ltd., Tao-Yuan, Taiwan, where he investigated related techniques on time and frequency synchronization. From 2004 to 2005, he worked as an Associate Engineer in the Multimedia Department of Northern Taiwan Business Group, Chunghwa Telecom Company, Ltd., and was responsible for the construction of multimedia-on-demand systems and interactive IPTV systems. Since 2006, he has been a faculty member of the Department of Electrical Engineering at Chang Gung University, Tao-Yuan, where he is currently an Associate Professor. His research interests include multimedia networks, digital right management, wireless networks, mobile IPTV, network synchronization, and smart home systems.

Hung-Ju Lin received the B.S and M.S. degrees in electrical engineering from the College of Engineering, Chang Gung University, Tao-Yuan, Taiwan, in 2010 and 2014, respectively.

Since 2014, he has been an Engineer with the Taiwan Power Company, Taipei, Taiwan. His research interests include electronic circuits, wireless sensor networks, power line communications, and smart home control systems.